Dynamic thermal modeling and parameter identification for a monolithic laser diode module*

Li Jin-Yi(李金义), Du Zhen-Hui(杜振辉)†, Ma Yi-Wen(马艺闻), and Xu Ke-Xin(徐可欣)

State Key Laboratory of Precision Measuring Technology and Instruments, Tianjin University, Tianjin 300072, *China*

(Received 22 July 2012; revised manuscript received 7 September 2012)

We improved the thermal equivalent-circuit model of the laser diode module (LDM) to evaluate its thermal dynamic properties and calculate the junction temperature of the laser diode with a high accuracy. The thermal parameters and the transient junction temperature of the LDM are modeled and obtained according to the temperature of the thermistor integrated in the module. Our improved thermal model is verified indirectly by monitoring the emission wavelength of the laser diode against gas absorption lines, and several thermal parameters are obtained with the temperature uncertainty of 0.01 K in the thermal dynamic process.

Keywords: laser diode module, dynamic thermal modeling, thermal time constant, tunable diode laser absorption spectroscopy (TDLAS)

PACS: 42.55.Px, 42.60.Fc **DOI:** 10.1088/1674-1056/22/3/034203

1. Introduction

The junction temperature of diode lasers affects their emitting efficiency, spectral characteristics, stability, and life time. For high-power laser diodes (LDs), researchers concentrated on understanding the effects of heavy thermal loss in the physical properties of the device.[1–6] For tunable diode lasers which are mostly used in coherent measurements and spectroscopy, an increasing number of thermal studies are dedicated to emission spectral characteristics which need higher measurement fidelity and resolution.[7–9] In spectroscopy and optical coherence measurements, a wavelength resolution of several pico-meters and a temperature resolution of 0.05 K are necessary for distributed feedback (DFB) lasers.[10]

For steady-state analysis of the thermal characteristics of LDs, thermal impedance is the most useful indicator. Feng *et al.* calculated the thermal impedances of the package materials of GaN LDs in a TO 56 package, and analyzed the effects of various thermal parameters on the thermal characteristics.[11] For the analysis of thermal dynamic properties of LDs, the thermal time constant is one of the most important parameters.[12–14] Mulvihill and O'Dowd reviewed the thermal transient measurement of grating-coupled rear reflector sampled lasers excellently and demonstrated a method to model a widely tuned laser used in the optically switched network.[15] However, the reliability of thermal parameters is virtually dependent on the measurement accuracy of the transient junction temperature of the laser diode, which is usually measured by the junction voltage[2–4] with an uncertainty of about 0.5 K.[4] The junction temperature of the laser diode can also be tracked by monitoring the emission wavelength of the laser diode with a higher accuracy. However, this is limited by the poor wavelength resolution (tens of pico-meters) of the spectrometer in real experiments.[14]

In this paper, we improve the thermal equivalent-circuit model of the LDM, and model the thermal time constants across the laser chip to the carrier, to the thermoelectric cooler (TEC), and to the LDM housing. The transient junction temperature of the laser diode is measured indirectly by the temperature of thermistor. Our result is verified by monitoring the emission wavelength against the gas absorption lines with an accuracy of 0.1 pm,[16] corresponding to a temperature accuracy of above 0.01 K for DFB lasers.

2. Model and method

In the standard butterfly package, a laser chip, a photo diode (PD), and a thermistor are all mounted onto a metal carrier, which is soldered with the cold side of a TEC. The hot side of the TEC is attached to the bottom of the housing. Figure 1 shows the configuration of the DFB laser with the butterfly package.

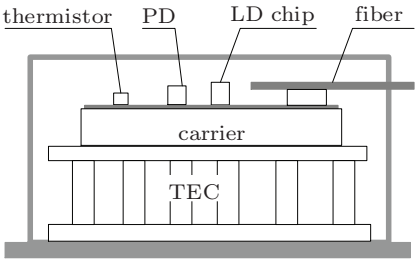


Fig. 1. Configuration of DFB laser with the butterfly package.

*Project supported by the Key Program of the National Natural Science Foundation of China (Grant No. 60938002), the Special-funded Program on National Key Scientific Instruments and Equipment Development of China (Grant No. 2012YQ06016501), and the Tianjin Research Program of Application Foundation and Advanced Technology, China (Grant No. 11JCYBJC04900).

†Corresponding author. E-mail: duzhenhui@tju.edu.cn

© 2013 Chinese Physical Society and IOP Publishing Ltd

2.1. Model of LDM

A thermal characteristics model described by the electronic component was used for the heat transfer analysis and the thermal control of the LDM. Lineykin[17] and Wey[18] developed a personal simulation program with an integrated circuit emphasis (PSPICE) compatible equivalent-circuit of the TEC to analyze its thermal performance. Mitrani[19] proposed a one-dimensional distributed parameter transient model for thermoelectric devices implemented by analogies between the thermal and electrical domains, where thermal variables are described by the corresponding electrical analogues. Through an equivalent electrical network, Yang *et al.*[20] analyzed the temperature control of the LDM by TEC, and demonstrated the steady state of the device.

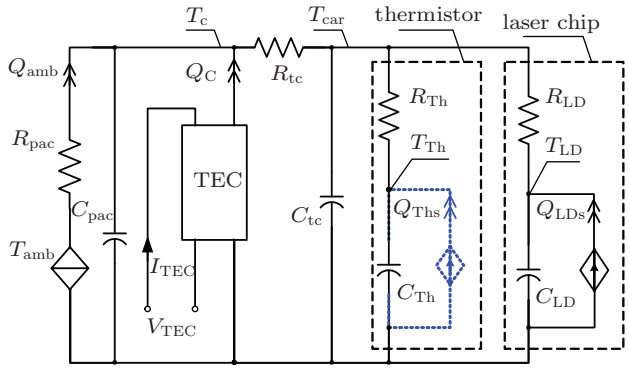


Fig. 2. (color online) Thermodynamics model of the LDM with a butterfly package.

Table 1. Nomenclature of symbols in Fig. 2.

Symbol	Meaning
T_{amb}/K	ambient temperature
R_{pac}/K·W[1]	thermal impedance of house to TEC cold side
C_{pac}/J·K^{-1}	thermal capacity of house to TEC cold side
Q_{amb}/W	heat induced by T_{amb} through R_{pac}
I_{TEC}/A	drive current of TEC
V_{TEC}/V	voltage of TEC
Q_c/W	heat induced by TEC through TEC cold side to carrier
T_c/K	temperature of TEC cold side
R_{tc}/K·W^{-1}	thermal impedance of TEC cold side to carrier
C_{tc}/J·K^{-1}	thermal capacity of TEC cold side to carrier
R_{Th}/K·W^{-1}	thermal impedance of thermistor
C_{Th}/J·K^{-1}	thermal capacity of thermistor
T_{Th}/K	temperature of thermistor
R_{LD}/K·W^{-1}	thermal impedance of LD chip
C_{LD}/J·K^{-1}	thermal capacity of LD chip
T_{LD}/K	temperature of LD chip
Q_{LDs}/W	Joule heat of LD chip
Q_{Ths}/W	Joule heat of thermistor

In our paper, we consider all components integrated in the LDM with lumped parameters, including a laser chip, a TEC, a thermistor, and a carrier. The influence of the environmental temperature on the temperatures of the LD chip and the thermistor is mainly caused by the housing of the LDM through the TEC to the carrier. The heat radiation and heat transfer through the air are negligible. The improved comprehensive thermal equivalent circuit model of the LDM is shown in Fig. 2, and the nomenclature of the symbols in Fig. 2 is shown in Table 1.

2.2. Thermal equilibrium state

When LDM reaches a thermal equilibrium, the junction temperature of the laser diode is related to the temperature of the carrier and the waste heat power is dissipated in the laser chip as follows:

$$T_{LD} = T_{car} + R_{LD} Q_{LDs}, \tag{1}$$

where the waste heatQ_{LDs} is the thermal power dissipated in the junction, and is equal to the total power supplied to the junction subtracted by the power radiated optically in the laser's light output, namely,

$$Q_{LDs} = UI - P_0, \tag{2}$$

where U is the laser junction voltage in V, I is the laser injection current in A, and P_0 is the optical power of laser in W.

Similarly, according to the thermal equivalent circuit model, the temperature of the thermistor T_{Th} is expressed as

$$T_{Th} = T_{car} + R_{Th} Q_{Ths}, \tag{3}$$

where the spontaneous heat Q_{Ths} of the thermistor is dependent on its resistance and current. The current flowing through the thermistor is usually in the range from 0.1 mA to 0.05 mA, with a power dissipation of 10^{-4} W. The increase in temperature caused by the thermistor current is in the order of 10^{-3} K. Compared with the laser diode heat power dissipation of 10^{-2} W and the TEC heat power of several Watts, the thermal variation caused by the thermistor current is ignored. Therefore, equation (3) can be simplified for the thermal equilibrium state as

$$T_{Th} = T_{car}. \tag{4}$$

The thermal impedance of the carrier-to-laser chip can be derived from Eq. (1) combining with Eqs. (2) and (4).

2.3. Thermal dynamic process

The junction temperature of the laser diode is changed continuously in the thermal dynamic process actively by the TEC or passively by the surrounding environment. Under the coactions of the TEC and the surrounding environment, temperatures of the thermistor and the laser diode junction are guided by the following equation:

$$Q_{amb} + Q_C = C_{car} \frac{dT_{car}}{dt} + C_{Th} \frac{dT_{Th}}{dt} + C_{LD} \frac{dT_{LD}}{dt} - Q_{LDs}. \tag{5}$$

Since the variables in Eq. (5) are hard to measure, it is difficult to obtain the value of T_{LD}. Nevertheless, the relationship between the junction temperature of the laser diode

and the temperature of the thermistor can be established from another point of view. According to the thermal equivalent circuit model shown in Fig. 2, the relationship between the temperature of the thermistor, the junction temperature of the laser diode, and the temperature of the carrier are given by

$$R_{\rm Th}\cdot C_{\rm Th}\frac{{\rm d}T_{\rm Th}}{{\rm d}t}+T_{\rm Th}=T_{\rm car}, \tag{6}$$

$$R_{\rm LD}\cdot\left(C_{\rm LD}\frac{{\rm d}T_{\rm LD}}{{\rm d}t}-Q_{\rm LDs}\right)+T_{\rm LD}=T_{\rm car}, \tag{7}$$

during the thermal dynamic process. Combining Eq. (6) with Eq. (7), we can derive the differential equation

$$R_{\rm LD}C_{\rm LD}\frac{{\rm d}T_{\rm LD}}{{\rm d}t}+T_{\rm LD}=T_{\rm Th}+R_{\rm Th}C_{\rm Th}\frac{{\rm d}T_{\rm Th}}{{\rm d}t}+R_{\rm LD}Q_{\rm LDs}. \tag{8}$$

Regarding the right-hand side of Eq. (8) as an incentive of $T_{\rm LD}$, we obtain the total solutions of the differential equation (8) as

$$T_{\rm LD}=T_X+[T_{\rm LD}(0)-T_X]\,{\rm e}^{-t/\tau_{\rm LD}}, \tag{9}$$

$$T_X=T_{\rm Th}+\tau_{\rm Th}\frac{{\rm d}T_{\rm Th}}{{\rm d}t}+R_{\rm LD}Q_{\rm LDs}, \tag{10}$$

where $\tau_{\rm LD}=R_{\rm LD}C_{\rm LD}$ is the thermal time constant of the LD chip, $\tau_{\rm Th}=R_{\rm Th}C_{\rm Th}$ is the thermal time constant of the thermistor to the carrier, and $T_{\rm LD}(0)$ is the initial temperature of the junction satisfying

$$T_{\rm car}(0)=T_{\rm Th}(0)-R_{\rm Th}Q_{\rm Ths}(0)=T_{\rm LD}(0)-R_{\rm LD}Q_{\rm LDs}(0). \tag{11}$$

Therefore,

$$T_{\rm LD}(0)=T_{\rm Th}(0)-R_{\rm Th}Q_{\rm Ths}(0)+R_{\rm LD}Q_{\rm LDs}(0). \tag{12}$$

Substituting Eqs. (8) and (12) into Eq. (9), we obtain

$$\begin{aligned}T_{\rm LD}=&\left(T_{\rm Th}+\tau_{\rm Th}\frac{{\rm d}T_{\rm Th}}{{\rm d}t}+R_{\rm LD}Q_{\rm LDs}\right)(1-{\rm e}^{-t/\tau_{\rm LD}})\\&+[T_{\rm Th}(0)+R_{\rm LD}Q_{\rm LDs}(0)]\,{\rm e}^{-t/\tau_{\rm LD}}.\end{aligned} \tag{13}$$

According to Eq. (13), we can obtain the time constants of the LD chip and the thermistor by the junction temperature of the laser diode ($T_{\rm LD}$), the temperature of thermistor ($T_{\rm Th}$), and the waste heat power of the LD chip ($Q_{\rm LDs}$) during the thermal dynamic process.

In similar manner, we can deduce the temperature of the carrier $T_{\rm car}$ as

$$T_{\rm car}=T_{\rm amb}\cdot(1-{\rm e}^{-t/\tau_{\rm c}})+T_{\rm car}(0)\,{\rm e}^{-t/\tau_{\rm c}}, \tag{14}$$

where $T_{\rm car}(0)$ is the initial temperature of carrier ($t=0$), and $\tau_{\rm c}=R_{\rm pac}C_{\rm pac}$ is the thermal time constant of the carrier to the housing.

2.4. Thermal parameters

The authors of Refs. [16]– [19] have investigated the transient performances of thermoelectric coolers, from which we can conclude that the step response of the temperature of the cold side of the TEC in heating mode is approximately linear with time at a constant temperature of heat sink combined with the hot side of the TEC and within a short time t ($t\ll t_{\rm r}$). Here, $t_{\rm r}$ (the response time of the TEC) is the duration time that the temperature difference ΔT between the cold side and the hot side of the TEC increases from zero to a stable value $\Delta T_{\rm max}$ under a constant TEC drive current.

For general TECs, the response time is about tens of seconds,[21] whereas the time of the temperature rise is less than 1 s. Hence, the temperature $T_{\rm c}$ of the cold side of the TEC varies linearly with time under a constant negative drive current as follows:

$$T_{\rm c}\approx kt+T_{\rm c}(0), \tag{15}$$

where k is the slope of the temperature variation over time, which increases with the absolute value of the TEC current, and $T_{\rm c}(0)$ is the initial temperature of the cold side of the TEC. Therefore, in this case, the slope response of the carrier temperature can be expressed as

$$T_{\rm car}=k(t-\tau_{\rm tc}+\tau_{\rm tc}\,{\rm e}^{-t/\tau_{\rm tc}})+T_{\rm c}(0), \tag{16}$$

where $\tau_{\rm tc}$ is the thermal time constant of the cold side of the TEC to the carrier, which is defined by $\tau_{\rm tc}=R_{\rm tc}C_{\rm tc}$. Thus, we can derive it from Eq. (16). By setting various TEC currents, we can also derive $\tau_{\rm c}$ according to Eq. (14).

3. Experimental system

A commercial DFB laser with a nominal wavelength of 1.580 μm was used as the test object. The laser diode was housed in a butterfly-type 14 pin package with TEC and NTC thermistor. The bottom surface of the carrier was either cooled or heated by the TEC. The heat flowed through the carrier and was then absorbed by the TEC, so that the LD chip could be maintained at a low constant temperature. In addition, the LD chip could be heated by adding a reverse step current to the TEC to achieve temperature tuning.

The absorption lines of carbon dioxide (CO_2) in the band within the tuning range of the LD were selected to be an accurate wavelength marker. The experimental system was based on a tunable diode laser spectroscopy (TDLAS), as shown in Fig. 3. The laser injection current, the TEC driving current, and the thermistor current are all provided by a laser controller (ILX: LDC-3908). The signal generator provided a laser modulation signal and a reference for demodulation. A multi-path cell was filled with 10% CO_2/N_2 gas mixture. The signals of gas absorption and thermistor voltage were recorded and then

processed by a computer. The detailed experimental system has been presented in our previous paper.[22]

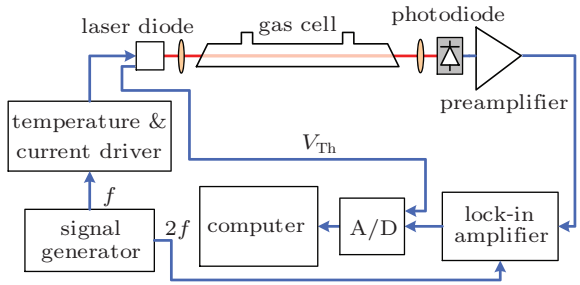


Fig. 3. (color online) Schematic of experimental apparatus for $2f$-wavelength modulation spectroscopy (WMS).

4. Results and discussion

At the TEC driving current of -1 A, the range of the observed temperature of the thermistor scanned is between 266.58 K and 305.11 K. The WMS-$2f$ signal of the CO_2 absorption lines and the temperature of the thermistor versus time are shown in Fig. 4, which covers eight absorption lines. The wavelength of the eight lines can be found in a high-resolution transmission molecular absorption database (HITRAN),[23] which are shown in the first column of Table 2. The temperature of the thermistor, the temperature rate, and the time at each absorption peak were recorded simultaneously, are shown in the 2nd, 3rd, and 4th columns of Table 2, respectively.

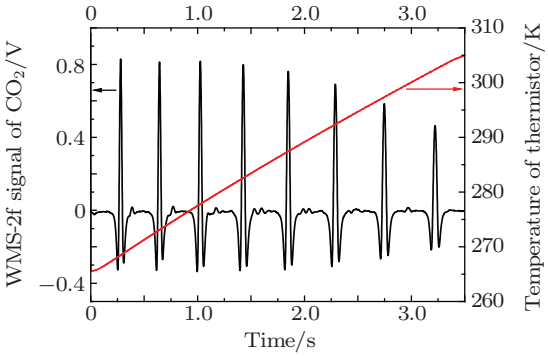


Fig. 4. (color online) A WMS-$2f$ signal of CO_2 and the temperature of the thermistor during the thermal tuning of the DFB laser (at an ambient temperature of 293.35 K and a gas pressure of 1 atm).

Moreover, the junction voltage and output power of the DFB laser were measured by optical spectrum analyzer (Agilent: 86142 B) at various temperatures. The collected data are shown in the 5th and 6th columns of Table 2. It is noticed from Table 2 that a higher temperature results in a higher threshold current and a reduced optical power, which is responsible for the dependency of the effective refractive index, the band gap energy, and the Fermi distribution to the temperature.[8] Waste thermal powers of the LD calculated according to Eq. (3) are shown in the 7th column of Table 2.

Table 2. Information of the thermistor and LD measured at each absorption peak. λ: wavelength of absorption lines of CO_2 in Hitran; U: junction voltage; P_o: output optical power; Q_{LDs}: waste thermal power.

λ/nm	T_{Th}/K	dT_{Th}/dt/K·s^{-1}	t/s	U/V	P_0/W	Q_{LDs}/W
1578.6653	268.353	12.275	0.2039	1.1103	0.01186	0.04365
1579.1158	272.965	12.304	0.5758	1.1077	0.01189	0.04350
1579.5739	277.681	11.880	0.9659	1.1055	0.01186	0.04342
1580.0395	282.468	11.445	1.3765	1.1037	0.01176	0.04342
1580.5127	287.313	11.100	1.8068	1.1023	0.01159	0.04352
1580.9933	292.242	10.747	2.2585	1.1012	0.01133	0.04373
1581.4814	297.235	10.464	2.7292	1.1005	0.01096	0.04406
1581.9770	302.281	10.204	3.2177	1.0998	0.01046	0.04453

According to Ref. [8], a linear relationship

$$\lambda = mT_{LD} + b \tag{17}$$

exists between the wavelength and the junction temperature of the laser diode. Substituting Eq. (13) into Eq. (17), we obtain

$$\lambda = m\left\{(T_{Th} + \tau_{Th}\frac{dT_{Th}}{dt} + R_{LD}Q_{LDs})(1 - e^{-t/\tau_{LD}}) + [T_{Th}(0) + R_{LD}Q_{LDs}(0)]\,e^{-t/\tau_{LD}}\right\} + b. \tag{18}$$

According to Eq. (18) and the data in Table 2, by means of multiple nonlinear least squares fitting, we obtained the carrier-to-chip thermal impedance as well as the time constants of the thermistor and LD chip, as shown in Table 3. The corresponding standard errors of the parameter estimates in the regression analysis are listed in the 4th column of Table 3. Once parameters m and b are identified, the laser wavelength λ can be determined according to Eq. (17) when the junction temperature of the laser diode T_{LD} is known, and vice versa. Here, according to the tuning characteristic, the dynamic junction temperature of the laser diode can be determined based on the measured wavelength of the LD. With known data in Tables 2 and 3, junction temperatures can be calculated according to Eqs. (13) and (17), respectively, indicating that the

deviations are less than 0.01 K.

Note that it is necessary to obtain the precise emission wavelength by means of Eq. (18) to estimate the parameters in Table 3, which is related to the model accuracy. There are some other ways to obtain a more precise wavelength. For example, the commercial wavemeters have a wavelength precision of less than 1 pm, but it is not suitable for this dynamic measurement. Optical frequency combs would give a continuous wavelength (frequency) with a higher accuracy. However, it is not only very expensive, but also could be only used under ultra-clean conditions. Hence, we adopted the gas absorption scheme and obtained high-precision dynamic wavelength information easily with lower cost.

Table 3. Thermal property of a DFB laser diode.

Parameter	Physical meaning	Value	Standard error
m/nm·K^{-1}	slope	0.09782	9.2×10^{-5}
b/nm	intercept	1552.0878	0.05764
$R_{\rm LD}$/K·W^{-1}	thermal impedance of LD chip	59.34	7.37
$\tau_{\rm Th}$/ms	time constant of the thermistor	61.73	17.41
$\tau_{\rm LD}$/ms	time constant of LD chip	3	–

Additionally, the laser injection current was turned off at room temperature and the thermal time constant of the carrier was measured. The LD controller was applied to ensure that the temperature of the LDM remains stable at 268.13 K, and then the TEC driving current was turned off. Changes in the temperature of the thermistor excited by the ambient temperature were recorded. According to Eq. (14), the thermal time constant of the housing-carrier was derived, which is shown in the 1st row of Table 4.

Table 4. Results of the thermal time constants.

Thermal time constant	symbol	Unit	Value	Standard Error
housing-carrier	$\tau_{\rm hc}$	s	14.69	0.02
TEC-carrier	$\tau_{\rm tc}$	ms	13.18	0.14

In order to determine $\tau_{\rm tc}$, the following experimental steps were introduced. When $t=0$, the temperature of the carrier was kept at 266.58 K, and a step drive current of -1 A was imposed on TEC. When $t>0$, the carrier was heated by the TEC due to a reversed current. The thermal excitation to the carrier is approximately a slope function of time t, which is shown in Fig. 5. The carrier was very thin (400 μm) and was made of aluminum nitride (AlN) with a good thermal conductivity (230 W·m^{-1}·K^{-1}). Therefore, the temperature grading inside the carrier could be neglected. By taking the cold side of the TEC and the carrier as a whole component, and according to Eq. (16), the thermal time $\tau_{\rm tc}$ of this component is estimated to be 13.18 ms with a standard error of 0.14 ms using the fitting method (see Fig. 5).

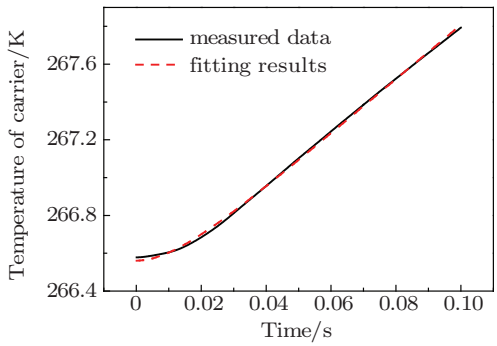


Fig. 5. (color online) The relationship between the carrier temperature and time.

Tables 3 and 4 show that the thermal time constant of the LD chip is the smallest one, which means that the LD chip transmits waste heat rapidly. The time constant of the thermistor is one order of magnitude higher than that of the LD chip. Therefore, the thermistor is unable to follow the rapid temperature variations of the junction and the carrier. In the LD temperature control system which is sensitive to temperature overshoot, it is particularly important to maintain good tracking between the temperature sensor and the temperature controller, and thus a smaller thermal mass thermistor is a better choice. The time constant of housing to carrier is the biggest one, which determines the effects of ambient temperature on the heat transfer process of the LD. The thermal time constant of the carrier to the cold side of the TEC is a very important parameter, which represents the time for the LD chip thermal power dissipating through the carrier to the cold side of the TEC during the temperature control and thermal tuning of the LD. This has two meanings. Firstly, the time constant determines that the theoretical precision of temperature control is about 10^{-4} K for a given thermal power of 20 mW. Secondly, it determines that the rate of thermal tuning is in the magnitude order of milliseconds. There are two reasons for the fact that the time constant of the TEC-carrier is smaller than that of the thermistor. (i) The contact area between the carrier and the cold side of TEC is about tens of times larger than that between the carrier and the thermistor. (ii) The pad of the carrier is AlN with a good thermal conductivity, which is soldered on the cold side of the TEC made of nickel with a thermal conductivity of 90 W·m^{-1}·K^{-1}, whereas the sub-mount of the thermistor is made of Al_2O_3 with a poor thermal conductivity (12 W·m^{-1}·K^{-1}).[24] Considering all these factors, we conclude that the thermal impedance of the thermistor to the carrier is larger than that of the carrier to the TEC, which results in a larger thermal time constant. The above thermal time constants are important in calculating the proportion integration differentiation (PID) controller parameters in a temperature control system.

5. Conclusion

For monolithic laser diodes, the spectral characteristics are more sensitive to temperature. Therefore, it becomes extremely necessary to study the thermal parameters of the LDM. In this paper, we used our method to calculate the thermal parameters of components in the LDM. Four experiments based on the equivalent circuit model of the LDM are designed, and five thermal parameters were obtained. They are the thermal time constants of the LD chip (3 ms), thermistor (61.73 ms), carrier to housing (14.7 s), and carrier to the cold side TEC (13.18 ms), respectively. In addition, the thermal impedance of the carrier-to-chip is 59.34 K/W. Compared with the previous work in Ref. [4], where a 0.5 K measurement accuracy was achieved for a DFB laser, an accuracy of 0.01 K or 50 times higher accuracy has been realized by means of the gas absorption line measurement in our work. The important condition for the model is that the thermistor and the LD chip must be attached onto the same carrier, which most packages can satisfy, such as TO, HHL, C-mount, butterfly, etc. Therefore, our method can be adapted to any other package by simply modifying the model parameters. The key point is to find the gas absorption lines corresponding to the emission wavelength of the measured LD.

Acknowledgements

The authors thank Dr. Xue Bin for his invaluable assistance and support.

References

[1] Ryabtsev G, Kuzmin A, Ges J, Gorban Y, Soukieh M, Konyaev V and Stręk W 1995 *J. Appl. Spectrosc.* **62** 900

[2] Ryu H, Ha K, Chae J, Nam O and Park Y 2005 *Appl. Phys. Lett.* **87** 093506

[3] Liu Y T, Cao Q, Song G F and Chen L H 2009 *Laser Phys.* **19** 400

[4] Kirkup L, Kalceff W and McCredie G 2007 *J. Appl. Spectrosc.* **101** 023118

[5] Jeong J H, Kim K C, Lee J I, Kim H J and Han I K 2008 *IEEE Photonic. Technol. Lett.* **20** 1354

[6] Liu X S, Hu M H, Caneau C G, Bhat R and Zah C E 2006 *IEEE Tran. Compon. Pack. Technol.* **29** 268

[7] Werle P 1998 *Spectrochimica. Acta Part A.* **54** 197

[8] Buus J, Amann M C and Blumenthal D J 2005 *Tunable Laser Diodes and Related Optical Sources* (2nd edn.) (New York: Wiley Press) p. 96

[9] An Y, Du Z H, Liu J W and Xu K X 2012 *Acta Phys. Sin.* **61** 034207 (in Chinese)

[10] Liu J W, Du Z H, Li J Y, Qi R B and Xu K X 2011 *Acta Phys. Sin.* **60** 074213 (in Chinese)

[11] Feng M X, Zhang S M, Jiang D S, Liu J P, Wang H, Zeng C, Li Z C, Wang H B, Wang F and Yang H 2012 *Chin. Phys. B* **21** 084209

[12] Mulvihill G and O'Dowd R 2005 *J. Lightwave Technol.* **23** 4101

[13] Zhou S and Zhang X P 2007 *IEEE Photonic. Technol. Lett.* **19** 683

[14] Chen C, Xin G F, Qu R H and Fang Z J 2006 *Opt. Commun.* **260** 223

[15] Franklin C F, Powell J D and Workman M L 1998 *Digital Control of Dynamic System* (3rd edn.) (Boston: Addison Wesley Longman Press) p. 56

[16] Gilbert S L, Swann W C and Dennis T 2001 *Proceedings of Laser Frequency Stabilization, Standards, Measurement, and Applications* **4269** 184

[17] Lineykin S and Ben-Yaakov S 2005 *IEEE Power Electron. Lett.* **3** 63

[18] Wey T 2006 *Proceedings of IEEE-NEWCAS* June 18–21, 2006 Gatineau, Canada **7** 277

[19] Mitrani D, Salazar J, Turo A, Garcia M J and Chavez J A 2009 *Microelectronic. J.* **40** 1398

[20] Yang M W and Zhou Z Y 2008 *Optoelectron. Lett.* **4** 180

[21] Gong C M, Chen Z, Wu Z, Chang G Q, Qian R M and Chen Y F 2006 *J. Semicond.* **27** 944

[22] Li J Y, Du Z H, Qi R B and Xu K X 2012 *Acta Opt. Sin.* **32** 0130004

[23] Rothman L S, Jacquemart D, Barbe A, *et al.* 2005 *J. Quant. Spectrosc. Radiat. Transfer* **96** 139

[24] Lindgren S, Ahlfeldt H, Kerzar B and Kjebon O 1996 *Proceedings of the 22nd European Conference on Optical Communication* September 15–19, 1996 Oslo, Norway, p. 97